Activator Carbamino Carbon to Inhibitor Phosphorus Internuclear Distances in Ribulose-1,5-bisphosphate Carboxylase/Oxygenase. A Solid-State NMR Study†

Delbert D. Mueller,*,‡ Asher Schmidt,§,|| Kirk L. Pappan,‡ Robert A. McKay,§ and Jacob Schaefer*,§

Department of Biochemistry, Willard Hall, Kansas State University, Manhattan, Kansas 66505-3702, and Department of Chemistry, Washington University, St. Louis, Missouri 63130

Received November 16, 1994; Revised Manuscript Received February 14, 1995⊗

ABSTRACT: Ribulose-1,5-bisphosphate carboxylase/oxygenase (Rubisco) is a hexadecamer of approximately 550 kDa in most organisms. Rotational-echo double-resonance (REDOR) and transfer-echo double-resonance (TEDOR) solid-state NMR were used to obtain the average internuclear distance between the 99% $^{13}CO_2$-labeled activator carbamino carbon to the phosphate phosphorus nuclei of active-site-bound 2-carboxy-D-arabinitol 1,5-bisphosphate (CABP), in freeze-quenched, lyophilized samples of confrey Rubisco. The distance 7.5 ± 0.5 Å determined by solid-state NMR is in agreement with the distance of 7.7 Å inferred from the crystal-structure coordinates for spinach Rubisco−CABP−CO_2−Mg^{2+} quaternary complex.

Ribulose-1,5-bisphosphate carboxylase/oxygenase (Rubisco)[1] [3-phospho-D-glycerate carboxylase (dimerizing), EC 4.1.1.39] is present in all photosynthetic organisms and some chemosynthetic bacteria. In higher organisms, it is a hexadecameric molecule comprised of eight large and eight small subunits with a molecular mass of about 550 kDa (McFadden, 1980). Rubisco catalyzes the fixation of CO_2 into RuBP, which produces two molecules of 3PGA to start the Calvin cycle. Alternatively, Rubisco can catalyze the addition of O_2 to RuBP, giving rise to one molecule of 3PGA and one of 2PG, which starts photorespiration (Bowes *et al.*, 1971; Andrews & Lorimer, 1987). Before Rubisco shows any activity, however, it must be activated by CO_2 and Mg^{2+} (Lorimer *et al.*, 1976) at a site distinct from the active site (Miziorko, 1979a,b; Lorimer, 1979) but probably contiguous with it (Pierce & Reddy, 1986). Both the activation and the catalytic sites are located on the large subunit (Miziorko & Lorimer, 1983). Thus, Rubisco is a critical part of the initial steps in carbon fixation that start the food chain process on earth and lead to a net utilization of atmospheric CO_2.

Crystal structures for spinach (Andersson *et al.*, 1989; Knight *et al.*, 1990), tobacco (Curmi *et al.*, 1992), and *Synechococcus* (Newman & Gutteridge, 1993) Rubisco showed that the principal structure was a barrel-shaped, hollow-core tetramer of large subunit dimers with four small subunits located at the top and four at the bottom of the barrel in grooves between the ends of the large subunit dimers. In addition, the minimum possible catalytic unit was shown to be a dimer of large subunits since a portion of the N-terminal region of each subunit in the pair interacted with the C-terminal end of an α/β-barrel domain of the other to complete the two active sites. That arrangement also occurred in *Rhodospirillum rubrum* Rubisco, the most primitive form known, which is a dimer of large subunits only (Lundqvist & Schneider, 1989, 1991a; Schneider *et al.*, 1986, 1989).

The active sites of Rubisco are funnel-shaped with the activation Lys^{201} residue at the bottom of the funnel within the α/β barrel. The carboxylate groups of Asp^{203} and Glu^{204} provide two of the protein ligands for the required Mg^{2+} ion which is located near the bottom center of the active site. Formation of activator carbamate provides the remaining protein monodentate carboxyl oxygen ligand. Active-site-bound RuBP and substrate analogs such as, for example, CABP span the wider end of the funnel-shaped crevice with phosphate binding sites on either side of the opening and above the divalent metal ion (Figure 1). In the activated *Synechococcus* Rubisco complex with CABP, the 2-carboxyl group along with the C2 and C3 hydroxyl groups of the inhibitor completes the octahedral coordination of Mg^{2+}.

Upon binding of CABP to spinach Rubisco, a portion of the C-terminal loop 6 (Val^{334} to Ser^{341}) of the α/β barrel apparently moves over the active site, virtually excluding it and the CABP molecule from contact with solvent (Andersson *et al.*, 1989). That loop was either disordered or swung away from the active site in the crystal structures of *Rh. rubrum* Rubisco in several different states (Lundqvist & Schneider, 1991b) and in crystals of unactivated tobacco Rubisco with two sulfate, or phosphate, anions bound at the phosphate subsites (Chapman *et al.*, 1987; Curmi *et al.*, 1992). The highly polar active site appears well solvated in the unactivated open conformation (Curmi *et al.*, 1992). Seven extensively H-bonded water molecules are retained in the closed active site in the crystal structure of activated, CABP-complexed *Synechococcus* Rubisco (Newman & Gutteridge, 1993).

† This research was supported by NIH Grant GM40634 (J.S.) and by the Kansas Agricultural Experiment Station (D.D.M. and K.L.P. Contribution Number 95-50-J).

* Authors to whom correspondence should be addressed.

‡ Kansas State University.

§ Washington University.

|| Current address: Department of Chemistry, Technion−Israel Institute of Technology, Haifa 32000, Israel.

⊗ Abstract published in *Advance ACS Abstracts,* April 1, 1995.

[1] Abbreviations: Rubisco, ribulose-1,5-bisphosphate carboxylase/oxygenase; RuBP, ribulose 1,5-bisphosphate; 3PGA, 3-phospho-D-glyceric acid; 2PG, 2-phosphoglycolate; CABP, 2-carboxy-D-arabinitol 1,5-bisphosphate; Tris, tris(hydroxymethyl)aminomethane; DTT, dithiothreitol; EDTA, ethylenediaminetetraacetic acid; EPSP synthase, 5-*enol*-pyruvylshikimate-3-phosphate synthase; REDOR, rotational-echo double resonance; TEDOR, transfer-echo double resonance; CPMAS, cross-polarization magic angle spinning.

0006-2960/95/0434-5597$09.00/0

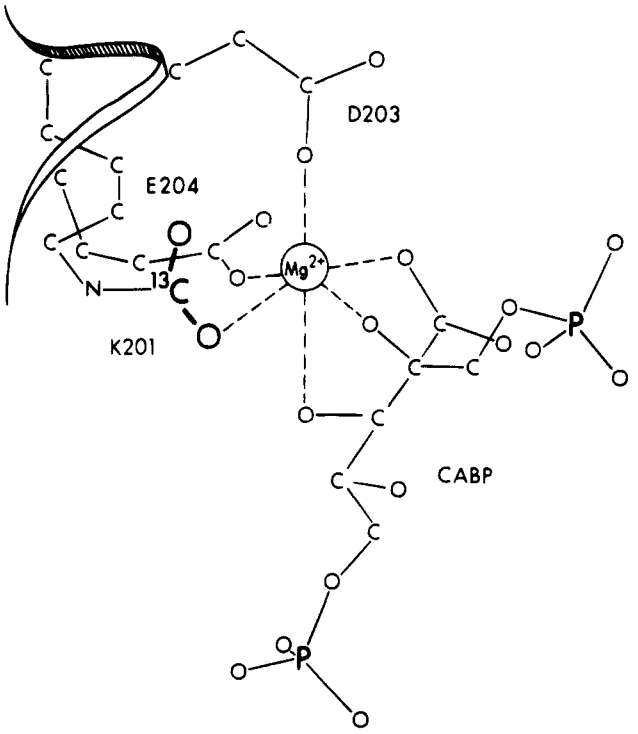

FIGURE 1: Schematic drawing of the binding site of Rubisco [adapted from Andersson *et al.* (1989)] showing that the C3 hydroxyl group of CABP is ligated to Mg^{2+} (Newman & Gutteridge, 1993).

Despite this wealth of information from crystallography, a number of critical questions remain. For example, the basic residue that initiates catalysis by extracting the hydrogen from carbon 3 of RuBP has yet to be unambiguously identified. In addition, it is not clear whether loop 6 of the α/β barrel closes during catalysis, although site-directed mutagenesis studies show that the strictly conserved Lys^{338} at the apex of loop 6 is important for activity (Chen & Spreitzer, 1989; Hartman & Lee, 1989; Gutteridge *et al.*, 1993).

NMR is an alternate method to X-ray diffraction for the study of molecular structure that potentially could provide answers to these and other questions. However, few solution-state NMR studies of Rubisco enzymes have been reported, probably because the size and, possibly, the solution stability of Rubisco limit potential experiments. With solid-state NMR, however, there is no resolution dependence on molecular weight and there is much less of a protein stability problem. One of these solid-state NMR methods, REDOR (Gullion & Schaefer, 1989a,b, 1991), allows accurate measurement of internuclear distances between heteronuclear pairs of spins over long distances: $^{13}C-^{15}N$, 6 Å; $^{13}C-^{31}P$, 10 Å; $^{13}C-^{19}F$, 12 Å; $^{31}P-^{19}F$, 15 Å. REDOR has been used to infer the following: (i) protein–catecholamine bond formation in insect cuticle development from $^{13}C-^{15}N$ distances (Christensen *et al.*, 1991); (ii) the geometry of ^{13}C-labeled inhibitors bound to EPSP synthase, a 46 kDa enzyme, from selected $^{13}C-^{31}P$ distances (Christensen & Schaefer, 1993); (iii) Trp–Trp distances among separately labeled ^{19}F and ^{13}C residues of cellular retinol binding protein II (McDowell *et al.*, 1993); (iv) peptide backbone conformations of helical emerimicin analogs (Marshall *et al.*, 1990) and melanostatin (Garbow & McWherter, 1993) from $^{13}C-^{15}N$ distances; (v) $[^{15}N]Ala_3-[^{13}C]Gly_2$ interresidue distances of gramicidin A in a model membrane system using two-dimensional REDOR (Hing & Schaefer, 1993); and (vi) the orientation of L-[5-^{13}C]glutamine in the binding site of [U-^{15}N]glutamine binding protein (Hing *et al.* 1994).

This study reports on the application of REDOR and TEDOR to confrey Rubisco to measure the average distance between the phosphates of active-site-bound CABP and the ^{13}C-labeled carbamino carbon of the activator CO_2. Comparison of the NMR-determined distance with the X-ray-determined distance is used to validate the REDOR methodology as applied to a large, multisubunit enzyme that has been freeze-quenched and lyophilized. This validation is a necessary first step to establish local geometry related to catalytic activity by the introduction of stable-isotope labels into Rubisco itself, and the subsequent measurement of distances between the enzyme and labeled substrates by REDOR.

EXPERIMENTAL PROCEDURES

Enzyme Preparation. Rubisco from comfrey (*Symphytum* spp.) leaves was isolated, stored, purified to electrophoretic homogeneity, activated, and assayed as described by Simpson *et al.* (1983) with minor modifications. First, in most cases, the excised leaves were immediately frozen in liquid N_2, and, secondly, 10 μM leupeptin was maintained throughout the procedure (Miller & Huffaker, 1982; Johal & Chollet, 1984; Rosichan & Huffaker, 1984; Servaites, 1985a). RuBP was prepared by the method of Horecker (1959) and purified by DEAE-cellulose column (6.5 × 1.2 cm) chromatography using 250 mL of 10–250 mM LiCl in a 1 mM HCl gradient after a 25 mL wash with 10 mM LiCl in 1 mM HCl. Excess LiCl was extracted from the lyophilized pooled 5 mL RuBP fractions with dry 8:1 acetone/methanol. The dried samples were redissolved in deionized water (pH adjusted to 6.5 with dilute NaOH), relyophilized, and stored sealed at −65 °C. Specific activities ranged from 1.0 to 1.7 μmol of $^{14}CO_2$ fixed min^{-1} (mg of protein)$^{-1}$.

Trapping and Stability of Activator CO_2. The extent of carbamylation of Lys^{201} by CO_2 was measured by CABP trapping of $^{14}CO_2$ into an exchange-inert quaternary CABP–$^{14}CO_2$–Mg^{2+}–Rubisco complex (Wishnick *et al.*, 1970; Miziorko 1979a,b; Miziorko & Sealy, 1980; Pierce *et al.*, 1980) using a slight modification of established procedures (Servaites, 1985b). Following elution of the enzyme from the DEAE-cellulose column with 50 mM Tris-HCl, 10 mM $MgCl_2$, 1 mM EDTA, and 1 mM DTT, pH 7.95, buffer (buffer A) made 0.15 M in NaCl, the pooled Rubisco fractions were lyophilized and stored at −20 °C. Assays and A_{280} measurements of the pooled fractions before and after lyophilization and resolution in buffer A consistently indicated no loss of specific activity and complete recovery of protein at enzyme concentrations ranging from 0.2 to 10 mg/mL. In contrast, lyophilization from buffer A of activated (20 mM $NaHCO_3$ added) enzyme, and especially of unactivated enzyme, resulted in less than full recovery of protein and usually some loss of specific activity as well. Redissolved enzyme lyophilized from buffer A + 0.15 M NaCl was deactivated by overnight dialysis in sealed cylinders at 4 °C against 2 L of buffer A that had been continuously purged in the presence of the sample for 2–3 h at room temperature with CO_2-free N_2. This procedure not only essentially completely reverses activator carbamate formation but also results in full recovery of protein and

frequently gives slightly increased specific activities, possibly from removal of some residual low molecular weight inhibitory compounds. Approximately 1 or 10 mg/mL solutions of deactivated Rubisco were reactivated for 45 min with various amounts of $NaHCO_3$ containing $NaH^{14}CO_3$ (New England Nuclear, specific activity 7.0 Ci/mol) in buffer A at 25 °C. Afterward, a 0.5−1.8 molar ratio of CABP to active sites was added and the mixture incubated at 30−32 °C for 30−45 min. After an additional 1−2 h at 25 °C, the samples were exhaustively dialyzed at 4 °C against one of several CO_2-free, N_2-purged buffers. After ≈24 h, with one change of dialysate buffer at 12 h, aliquots of the CABP−$^{14}CO_2$−Mg^{2+}−Rubisco solutions were analyzed for activator $^{14}CO_2$ by scintillation counting and for protein using the measured extinction coefficient of 1.7 mL mg^{-1} cm^{-1} at 280 nm for comfrey Rubisco (Bolden & Mueller, 1983). In some cases, dialyses were performed for up to 5 days.

To confirm the stability of the complex to lyophilization, the remaining dialyzed sample was divided into 1 mL portions, shell-frozen in 1.8 mL cryotubes in a dry ice/2-propanol, or liquid N_2, bath, and lyophilized for 8−16 h. This procedure typically produced powders with 8−16% water based on final weights. Subsequently, some of the dried samples were redissolved in the original volume of buffer and analyzed for recovery of protein and retention of activator $^{14}CO_2$. Other lyophilized samples were stored sealed in the cryotubes for different periods of time and at various temperatures before performing the same analyses.

Preparation of CABP−$^{13}CO_2$−Mg^{2+}−Rubisco for NMR. Samples of CABP-complexed activated Rubisco for solid-state NMR experiments were prepared as described above except that the concentration of enzyme during activation was always near 10 mg/mL, the activation mixture was made 20 mM in 99% $NaH^{13}CO_3$, and the molar ratio of CABP to active sites was held at 1.2:1. The complexed samples were exhaustively dialyzed against, and lyophilized from, a 10 mM Tris-HCl, 5 mM $MgCl_2$, and 1 mM DTT, pH 7.95 (buffer B) solution to which 0.2 g/L of Chelex-100 was added during dialysis. A sample using natural-abundance $NaHCO_3$ was prepared similarly. The lyophilized samples were stored at either −20 °C or −65 °C before being loaded into the NMR rotor. The specific sample used for analytical distance measurements was processed from two enzyme preparations, one with a specific activity of 1.50 IU and the other with 1.68 IU.

Solid-State NMR Experiments. Samples were packed into high-performance 7-mm zirconia rotors fitted with Kel-F spacers and drive cap. Cross-polarization, magic-angle spinning spectra were obtained at 121.3 MHz on a Chemagnetics spectrometer (Fort Collins, CO) using a home-built four-channel (^{1}H, ^{31}P, ^{13}C, ^{15}N) probe. The single, 9-mm inside diameter radiofrequency coil was connected by a low-loss transmission line to a quadruple-resonance tuning circuit outside the magnet (McKay, 1984). Cross-polarization transfers were performed at 50 kHz and proton decoupling at 90 kHz with a sequence repetition time of 2 s. The magic-angle stators were obtained from Chemagnetics (Fort Collins, CO). Controlled spinning speeds of either 5000 or 6024 Hz were used. Spectra were acquired with a temperature of 0 ± 2 °C over a 2-week period.

The carbon-observe, phosphorus-dephase REDOR pulse sequence (Figure 2) utilized pulses on both carbon and phosphorus channels, with the ^{13}C π pulses at the completion

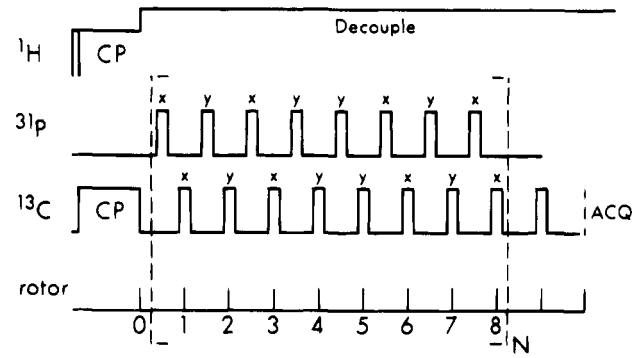

FIGURE 2: Pulse sequence for REDOR ^{13}C NMR with ^{31}P dephasing. The initial carbon magnetization arises from a matached spin-lock, proton-carbon transfer. The phases of carbon and phosphorus π pulses follow the xy-8 cycling scheme.

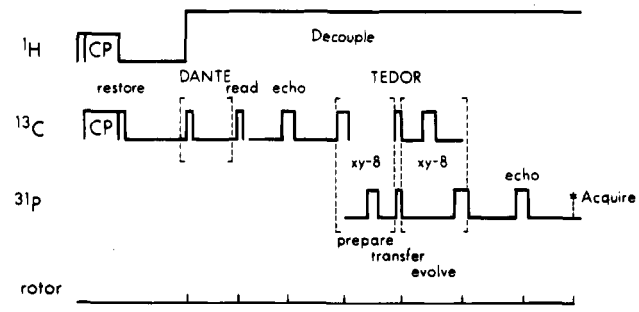

FIGURE 3: Pulse sequence for DANTE-selected, carbon-to-phosphorus, TEDOR NMR.

of each rotor period (to refocus isotropic chemical shifts), and the ^{31}P π pulses at each half-rotor period. These pulses were phase-cycled using the xy-8 scheme to eliminate resonance offset effects (Gullion *et al.*, 1990; Gullion & Schaefer, 1991). The ^{31}P π pulses cause a net dephasing of the transverse magnetization for ^{13}C nuclei dipolar-coupled to ^{31}P nuclei. This results in a REDOR difference signal, ΔS, between ^{13}C rotational-echo spectra obtained with and without dephasing ^{31}P pulses (Figure 2). The spectrum without ^{31}P pulses represents the full-echo signal, S_0. The ratio $\Delta S/S_0$ depends on the product of the number of rotor cycles of dephasing, the rotor period, and the dipolar coupling constant, D. The measured $\Delta S/S_0$ is compared to a value calculated (Olejniczak *et al.*, 1984) from a geometric model relating ^{13}C−^{31}P internuclear distances and D, which is equal to $\gamma_P\gamma_C h/2\pi r^3$, where γ_P and γ_C are the magnetogyric ratios of ^{31}P and ^{13}C, respectively, h is Planck's constant, and r is the internuclear distance. The experimental $\Delta S/S_0$ therefore determines D, and D determines r. A 5% reduction in D due to averaging by ultra-high-speed small-amplitude motion was assumed (Marshall *et al.*, 1990).

Transferred-echo double-resonance (TEDOR) experiments (Hing *et al.*, 1993) utilized selective DANTE inversion (first bracket, Figure 3) of the ^{13}C-labeled carbamate peak on alternate scans. The transverse magnetization of the carbamate peak therefore alternated in sign following the $\pi/2$ read pulse, as did the bilinear coherence developed by the π pulses of the preparation sequence (second bracket, Figure 3) for phosphorus dipolar-coupled to the 99% ^{13}C of the carbamate peak. Following coherence transfer by the coincident ^{13}C and ^{31}P $\pi/2$ pulses, the observed ^{31}P magnetization that evolved (third bracket, Figure 3) was refocused and alternated in sign from one scan to the next. Alternate scans were stored in separate buffers. The sum gave a ^{31}P

Table 1: Stability of Dialyzed CABP−Mg^{2+}−$^{14}CO_2$−Comfrey Rubisco to Lyophilization

activation conditions			lyophilized samples		
activation [$NaHCO_3$] (mM)	[Mg^{2+}] (mM)	CABP:site molar ratio	% protein recovered	CO_2:site molar ratio[b] initial	final
20.2	5	none		<0.002	
9.4	5	0.52		0.52	
21.4	5	1.2	107	1.02	0.93
21.4	1	1.2	103	0.78	0.56
2.1	5	1.8	94	0.92	0.93
5.25	5	1.8	103	1.14	1.12
10.5	5	1.8	103	1.27	1.20

[a] From the absorbance at 280 nm 2−5 min after redissolving the sample. [b] From the ^{14}C dpm of the redissolved sample and the specific radioactivity of the $NaHCO_3$ mixture.

signal arising from all phosphorus dipolar-coupled to ^{13}C (including natural-abundance ^{13}C), and the difference gave a ^{31}P signal arising only from phosphorus dipolar-coupled to the carbamate ^{13}C label.

RESULTS

Stability of CABP−$^{14}CO_2$−Mg^{2+}−Rubisco. Samples of CABP−$^{14}CO_2$−Mg^{2+}−Rubisco dialyzed at 4 °C for up to 5 days showed no further loss of dpm after the first 12 h in either 50 or 10 mM Tris-HCl buffers containing 5 or 10 mM $MgCl_2$ (buffers A or B, data not shown). This indicates that CABP formed an "exchange inert" complex with comfrey Rubisco. This complex was not, however stable to dialysis against 2 mM Tris-HCl, 1 mM $MgCl_2$, 1 mM DTT, and 0.4 μM bacitracin, pH 7.95, to which 0.2 g of Chelex-100/L was added (buffer C, data not shown). It appears that the Mg^{2+} concentration is the main stability-determining factor in solution. Samples dialyzed at 5 mM Mg^{2+} also were stable to shell-freezing and lyophilization as evidenced by >96% average retention of $^{14}CO_2$ relative to the dialyzed (initial) dpm (Table 1). The data in Table 1 also show that the amount of activator CO_2 trapped was essentially directly proportional to the molar ratio of CABP to active sites up to 1.2:1.

The amount of CO_2 trapped over a 2−3 h incubation with 1.8:1 CABP/active sites and 5 mM Mg^{2+} was independent of the initial degree of activation (Table 1). However, for reasons that are not yet clear, the data for 1.8:1 ratios of inhibitor consistently indicated retention of slightly more than one CO_2 per active site. Samples for NMR were prepared with a 1.2:1 ratio of CABP to active sites.

Virtually 100% of the dialyzed protein content was recoverable within 2 min of the addition of buffer to the lyophilized material (Table 1). Specific activities of the dialyzed and lyophilized complex were still 96−98% inhibited. Together those results suggest that the complex remained intact throughout sample preparation and that a large excess of RuBP substrate was unable to chase CABP from the active site, even after lyophilization and resolubilization. The stability of the dried complex to long-term storage in sealed cryotubes, however, was temperature-dependent (Table 2).

Carbon-Observe, Phosphorus-Dephase REDOR. The full-echo ^{13}C NMR of CABP−$^{13}CO_2$−Mg^{2+}−Rubisco has a narrow, chemical-shift resolved carbamate peak at 166 ppm (Figure 4, bottom) which was absent in the spectrum of the corresponding natural-abundance sample (data not shown).

Table 2: Long-Term Stability of Dialyzed and Lyophilized CABP−Mg^{2+}−$^{14}CO_2$−Comfrey Rubisco

activation [Mg^{2+}] (mM)	CABP/ sites	storage temp (°C)	time (days)	CO_2/ site	% retained[a]
1	1.2		0	0.56	(100)
		RT	35	0.32	57
		−65	35	0.62	111
5	1.2		0	0.93	(100)
		RT	35	0.33	35
		−65	35	0.93	100
5	1.2		0	0.69	(100)
		RT	20	0.37	39
		4	20	0.55	84
		−20	20	0.50	78
		−65	20	0.58	91

[a] All except the 20 day room temperature (RT) sample redissolved completely (93−110% recovery) within 2−5 min of adding the original buffer based on the absorbance at 280 nm.

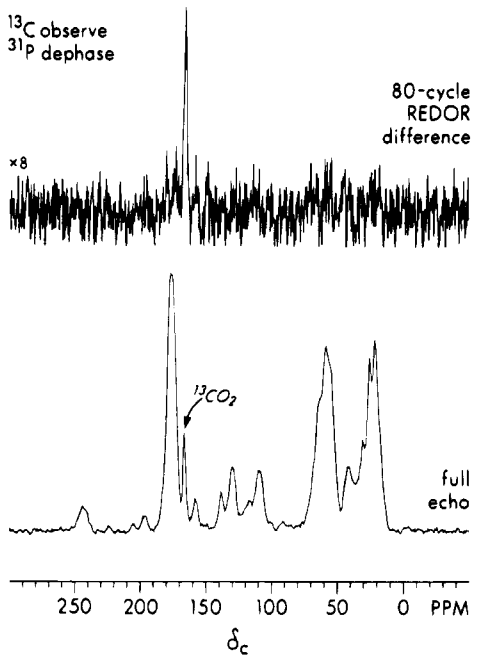

FIGURE 4: 75-MHz REDOR ^{13}C NMR full-echo spectrum (bottom) and difference spectrum (top) of a lyophilized CABP−$^{13}CO_2$−Mg^{2+}−comfrey Rubisco complex after 80 rotor cycles of ^{31}P dephasing at 5 kHz.

The sample for this experiment was freshly prepared and kept below 0 °C until it was loaded into the rotor. The extent of $^{13}CO_2$ incorporation into the complex was estimated by spin-count analysis utilizing the natural-abuandance protein carbonyl carbon peak centered at 175 ppm as an internal standard. The amino acid sequence of spinach Rubisco indicated 707 carbonyl carbons per protomer (1 large + 1 small subunit), and the corresponding number for comfrey Rubisco is not likely to differ by more than a few percent since there is nearly 95% sequence homology among the large subunits of higher plant Rubiscos. This implies a ratio of the natural-abundance carbonyl carbon peak intensity to 99% [^{13}C]carbamate peak intensity of 7.86:1 for one $^{13}CO_2$ carbamate/active site. The observed ratio is 7.02 (Figure 4, bottom), uncorrected for the slightly better echo refocusing of the $^{13}CO_2$ peak. Thus, ^{13}C NMR indicates essentially a 1:1 [^{13}C]carbamate:Rubisco active site ratio. A parallel $^{14}CO_2$ incorporation experiment for the same Rubisco preparation indicated 93% of theoretical carbamate formation under the same conditions.

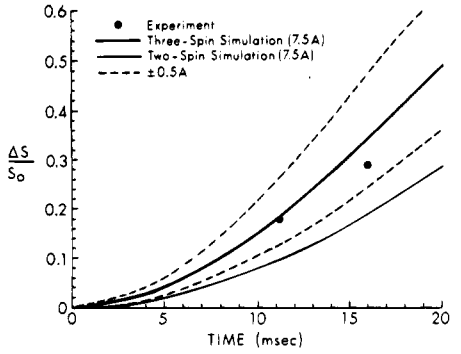

FIGURE 5: REDOR dephasing calculated for ^{13}C equidistant to two ^{31}P with a P−C−P subtended angle of 90°. Experimental dephasing for the CABP−$^{13}CO_2$−Mg^{2+}−Rubisco complex (solid circles) under 5 kHz magic-angle spinning (see Figure 4) suggests a 24 Hz dipolar coupling corresponding to a 7.5 Å ^{13}C−^{31}P distance (boldface line) with ±0.5 Å undertainty (dashed lines). REDOR dephasing calculated for a single ^{31}P at 7.5 Å from ^{13}C is reduced by about a factor of 2 (solid line). The experimentally determined dephasing near 11 ms is more reliable than that near 16 ms because of greater signal intensity.

The carbon-observe, phosphorus-dephase REDOR difference spectrum of CABP−$^{13}CO_2$−Mg^{2+}−Rubisco at 0 ± 2 °C for N_c = 80 has one peak arising from the ^{13}C-labeled carbamino carbon at 166 ppm (Figure 4, top). Contributions to the REDOR difference from natural-abundance ^{13}C in both CABP and protein are distributed over the entire spectrum and are not significantly above the noise. The observed $\Delta S/S_0$ values for the carbamate peak are 0.18 and 0.29 at N_c = 56 and N_c = 80, respectively. Since two phosphorus nuclei contribute to dephasing of the labeled carbamino carbon, a geometric model is needed to translate the observed dephasing into a distance. Such a model was obtained from the crystal structure coordinates (Brookhaven Protein Data Bank) of the CABP−$^{13}CO_2$−Mg^{2+}−spinach Rubisco complex. These coordinates indicated that the angle subtended by the carbamino carbon and the two nearly equidistant phosphate phosphorus atoms of CABP is approximately 90° (Figure 1). The theoretical three-spin dephasing curve (Olejniczak, *et al.*, 1984) giving the best fit to the two experimental $\Delta S/S_0$ values has an average ^{13}C to ^{31}P distance of 7.5 Å (Figure 5, solid boldface line).

Carbon-to-Phosphorus TEDOR. The proton−phosphorus CPMAS ^{31}P NMR spectrum of CABP in the enyzme complex has a narrow, 2 ppm wide line with a shifted, broad, high-field component which represents about 20% of the total intensity (Figure 6, top). This spectrum was obtained on the same sample that was used for the REDOR experiments after about 2 months of storage at −20 °C. Averaged center-peak ^{31}P spin counts as a function of cross-polarization time for the Rubisco quaternary complex were compared to similarly acquired data for a phosphoserine solid-powder standard. That result, in agreement with the $^{14}CO_2$ trapping and full-echo ^{13}C NMR data, indicates one CABP per active site (Table 3). A nearly identical amount (1.72 μmol of CABP) was found when the first spinning side-bands were included in both the standard and analytical sample intensity data. Samples of comfrey Rubisco without CABP had no detectable endogenous phosphorus (Table 3). The ^{31}P NMR spectrum resulting from a coherence transfer from all dipolar-coupled ^{13}C spins (labeled $^{13}CO_2$, and natural-abundance ^{13}C in CABP and protein, Figure 6, middle) has the same shape as the proton−phosphorus CPMAS ^{31}P NMR spectrum

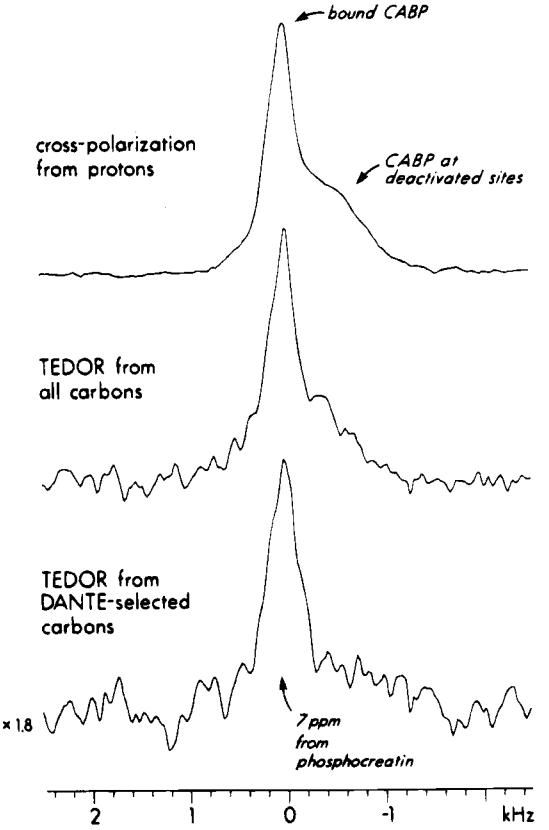

FIGURE 6: 121-MHz ^{31}P NMR spectra of a lyophilized CABP−$^{13}CO_2$−Mg^{2+}−Rubisco complex following a matached spin-lock transfer from protons (top), a TEDOR coherence transfer from all ^{13}C (middle), and a DANTE-selected TEDOR coherence transfer from bound $^{13}CO_2$ (bottom). The TEDOR spectra involved 32 rotor cycles of preparation and 48 cycles of evolution prior to data acquisition (see Figure 3). Magic-angle spinning was at 6024 Hz.

Table 3: ^{31}P Solid-State NMR Analysis of CABP Retained in Exhaustively Dialyzed and Lyophilized Rubisco Samples at 0 °C

sample	scans	integrated intensity per scan at 0 contact time	phosphorus (μmol)	active sites (μmol)[a]	CABP retained (μmol)
phosphoserine[b]	1024	4.43×10^{-5}	15		
CABP−Rubisco[c] (110 mg)[d]	8192	9.58×10^{-6}	3.33	1.65	1.66
Rubisco (68 mg)	79872	nd	*ca.* 0		

[a] Based on a molecular mass of 537 400 daltons for comfrey Rubisco and eight active sites per molecule. [b] Standard phosphoserine was lyophilized from a solution containing 250 mg of lysozyme. [c] A parallel $^{14}CO_2$ incorporation experiment on the same enzyme preparation indicated a molar ratio of 0.93 $^{14}CO_2$/active site after lyophilization. [d] From the absorbance at 280 nm and an extinction coefficient of 1.7 mL mg^{-1} cm^{-1} for comfrey Rubisco.

(Figure 6, top). Both sharp and broad-line components are present. The spectrum resulting from a coherence transfer from just bound $^{13}CO_2$ has a reduced contribution from the broad-line component (Figure 6, bottom).

DISCUSSION

Complex Formation and Lyophilization. The theoretical maximum amount of activator $^{14}CO_2$ is trapped by CABP using as little as 5 mM $NaH^{14}CO_3$ in the incubation mixture (Table 1), even though nearly 20 mM is needed to achieve full activity of purified comfrey Rubisco at pH 7.5−8.0 (Simpson *et al.*, 1983). This result confirms the observation (Miziorko, 1979a,b; Miziorko & Sealy, 1980) that CABP

forms an exchange-inert complex with activated Rubisco after incubation for more than 30 min at >25 °C. The movement of loop 6 over the active site observed in the crystal structure of spinach CABP−CO_2−Mg^{2+}−Rubisco may be responsible for the slow isomerization that converts the initial conformation of activated Rubisco, which binds CABP reversibly, into a state where the inhibitor becomes essentially irreversibly bound. We also conclude that the CABP enzyme quaternary complex can be lyophilized from dilute buffer solutions with >95% retention of activator carbamate. The 10 mg/mL Rubisco concentration and the 10 mM Tris-HCl concentration of buffer B used for NMR sample preparation resulted in approximately 100 buffer molecules per protomer molecule in the lyophilized state. Thus, after freeze-quenching and lyophilization, each molecule of CABP−$^{13}CO_2$−Mg^{2+}-Rubisco is embedded in a buffer glass, thereby reducing potential aggregation and denaturation (Christensen & Schaefer, 1993). Low temperatures, however, are needed to prevent a slow loss of activator CO_2 during long-term storage of the dried samples (Table 2).

Carbamate Chemical Shift. Carbamates of amino acids and of myoglobin have ^{13}C chemical shifts at 164−166 ppm, upfield from the protein carbonyl carbon peak at ≈175 ppm and downfield from the $H^{13}CO_3^-/CO_3^{2-}$ resonance at ≈162 ppm (Morrow *et al.*, 1973, 1974). O'Leary *et al.* (1979) used solution-state NMR to show that dimeric *Rh. rubrum* Rubisco in 6.6 mM $H^{13}CO_3^-$ gave a broad peak at 164.9 ppm that was absent in samples without added HCO_3^-. Similarly, solid-state ^{13}C NMR of the hexadecameric comfrey Rubisco activated with $^{13}CO_2$ shows a sharp, well-resolved peak at 166 ppm due to the carbamino carbon. Because CABP−$^{13}CO_2$−Mg^{2+}−comfrey Rubisco was subjected to exhaustive dialysis in the absence of added HCO_3^- and atmospheric CO_2, the 166 ppm peak in the solid-state NMR spectra is an exclusive measure of activator-site carbamates. This conclusion is supported by the amount of $^{14}CO_2$ retained in the dried samples, and by ^{13}C spin counts, both of which indicate a carbamino carbon:active-site ratio which is close to 1:1. Finally, the sharpness of the 166 ppm activator CO_2 peak suggests that all eight active sites of comfrey provide the same chemical shift environment.

Sharp and Broad-Line ^{31}P NMR Components. The broad upfield shoulder apparent in the ^{31}P spectra of the quaternary complex (Figure 6, top) seems incompatible with the observation of a sharp, symmetrical [^{13}C]carbamate resonance (Figure 4, top). In addition, solution-state NMR of the same kind of complex with dimeric *Rh. rubrum* Rubisco had shown a single, broad, symmetrical ^{31}P peak (Pierce & Reddy, 1986). Because lyophilized quaternary complexes were readily and completely soluble in the original buffer (Table 1), it is unlikely that the broad ^{31}P NMR peak resulted from denaturation that released bound CABP. A variety of chemical shift environments for bound CABP phosphate(s) could arise from cooperative interactions among the subunits for which there is some evidence. From nondenaturing gel electrophoresis and isoelectric focusing behavior of spinach Rubisco as a function of the amount of bound CABP, Johal *et al.* (1985) concluded that active-site binding of the inhibitor showed negative cooperativity. In addition using gel permeation chromatography and CABP concentrations in excess of that needed to form the exchange-inert complex, Yokota *et al.* (1991) found allosteric-site binding that displayed positive cooperativity. In contrast to active-site binding, the allosteric-site binding was reversible, and, therefore, any CABP bound to those sites should have been removed by the exhaustive dialysis of the samples used in this study, which were prepared with only a 20% molar excess of CABP. If active-site cooperativity were responsible for the small, broad upfield feature in the ^{31}P spectrum, those effects were not evident in the sharp, symmetrical ^{13}C-labeled carbamate resonances. Thus, considering that activator CO_2 can slowly escape from lyophilized samples (Table 2), a more likely explanation for the upfield shoulder is that it represents native enzyme that lost 20% of activator $^{13}CO_2$ during handling, data acquisition, and the 2 months of storage at −20 °C, but retained CABP in a more loosely bound or disorganized state near the binding site. In that situation, a broad ^{31}P peak could result from a distribution of slightly different environments for the phosphate(s) in deactivated binding sites. Consistent with this explanation, the TEDOR coherence transfer results suggest that carbamate carbons are only near those inhibitor molecules associated with the sharp ^{31}P line component (Figure 6, bottom).

REDOR Distance Measurements in Rubisco Complexes. Because of ^{13}C−^{31}P REDOR distance determination is made with *carbon* observation, the minor loss of $^{13}CO_2$ discussed above is not crucial. All the remaining carbamate $^{13}CO_2$ has bound CABP ^{31}P nearby. The REDOR-measured average CABP phosphorus to carbamino carbon distance is 7.5 ± 0.5 Å for comfrey Rubisco (Figure 5). This value is indistinguishable from the 7.7 Å predicted from the crystal structure coordinates for the same quaternary complex of spinach Rubisco. The agreement between these two measurements proves that solid-state NMR techniques can be successfully applied to the analysis of lyophilized samples of high molecular weight oligomeric proteins such as Rubisco. The demonstration by NMR of an apparently undisturbed, native binding site also means that in addition to CABP, Mg^{2+}, and CO_2, the structurally important, active-site water molecules are probably retained in the lyophilized comfrey Rubisco quaternary complex.

ACKNOWLEDGMENT

D.D.M. thanks Professor Jacob Schaefer for his hospitality during a sabbatical leave to St. Louis. D.D.M. also thanks Dr. John Pierce, Central Research and Development Department, E. I. du Pont de Nemours and Co., Experimental Station, Wilmington, DE, for the kind gift of diasteromerically resolved CABP. The simulations of Figure 6 were performed by Dr. C. A. Klug, Department of Chemistry, Washington University.

REFERENCES

Andersson, I., Knight, S., Schneider, G., Lindqvist, Y., Lundqvist, T., Branden, C.-I., & Lorimer, G. H. (1989) *Nature (London) 337*, 229−234.

Andrews, T. J., & Lorimer, G. H. (1987) *Biochem. Plants 10*, 131−218.

Bolden, T. D., & Mueller, D. D. (1983) *Biochem. Int.* 6, 93−99.

Bowes, G., Ogren, W. L., & Hageman, R. H. (1971) *Biochem. Biophys. Res. Commun. 45*, 716−722.

Chapman, M. S., Suh, S. W., Cascio, D., Smith, W. W., & Eisenberg, D. (1987) *Nature 329*, 354−350.

Chen, Z., & Spreitzer, R. J. (1989) *J. Biol. Chem. 264*, 3053−3055.

Christensen, A. M., & Schaefer, J. (1993) *Biochemistry 32*, 2868−2873.
Christensen, A. M., Schaefer, A., Kramer, K. J., Morgan, T. D., & Hopkins, T. L. (1991) *J. Am. Chem. Soc. 113*, 6799−6802.
Curmi, P. M. G., Cascio, D., Sweet, R. M., Eisenberg, D., & Schreuder, H. (1992) *J. Biol. Chem. 267*, 16980−16989.
Garbow, J. R., & McWherter, C. A. (1993) *J. Am. Chem. Soc. 115*, 238−244.
Gullion, T., & Schaefer, J. (1989a) *J. Magn. Reson. 81*, 196−200.
Gullion, T., & Schaefer, J. (1989b) *Adv. Magn. Reson. 13*, 55−83.
Gullion, T., & Schaefer, J. (1991) *J. Magn. Reson. 92*, 439−442.
Gullion, T., Baker, D., & Conradi, M. S. (1990) *J. Magn. Reson. 89*, 479−482.
Gutteridge, S., Rhoades, D., & Herrmann, C. (1993) *J. Biol. Chem. 268*, 8718−8724.
Hartman, F. C., & Lee, R. (1989) *J. Biol. Chem. 264*, 11784−11789.
Hing, A. W., & Schaefer, J. (1993) *Biochemistry 32*, 7593−7604.
Hing, A. W., Tjandra, N., Cottam, P. F., Schaefer, J., & Ho, C. (1994) *Biochemistry 33*, 8651−8661.
Horecker, B. L., Hurwitz, J., & Weisbach, A. (1958) *Biochem. Prep. 6*, 83−90.
Johal, S., & Chollet, R. (1984) *Arch. Biochem. Biophys. 223*, 40−50.
Johal, S., Partridge, B. E., & Chollet, R. (1985) *J. Biol. Chem. 260*, 9894−9904.
Knight, S., Andersson, I., & Branden, C.-I. (1990) *J. Mol. Biol. 215*, 113−160.
Lorimer, G. H. (1979) *J. Biol. Chem. 254*, 5599−5601.
Lorimer, G. H., Badger, M. R., & Andrews, T. J. (1976) *Biochemistry 15*, 529−536.
Lundqvist, T., & Schneider, G. (1989) *J. Biol. Chem. 264*, 7078−7083.
Lundqvist, T., & Schneider, G. (1991a) *Biochemistry 30*, 904−908.
Lundqvist, T., & Schneider, G. (1991b) *J. Biol. Chem. 266*, 12604−12611.
Marshall, G. R., Beusen, D. D., Kociolek, K., Redlinski, A. S., Leplawy, M. T., Pan, Y., & Schaefer, J. (1990) *J. Am. Chem. Soc. 112*, 963−966.
McDowell, L. M., Holl, S. M., Qian, S., Li, E., & Schaefer, J. (1993) *Biochemistry 32*, 4560−4563.
McFadden, B. A. (1980) *Acc. Chem. Res. 13*, 394−399.
McKay, R. A. (1984) U.S. Patent 4446431.
Miller, B. L., & Huffaker, R. C. (1982) *Plant Physiol. 69*, 58−62.
Miziorko, H. M. (1979a) *J. Biol. Chem. 254*, 270−272.
Miziorko, H. M. (1979b) *J. Biol. Chem. 254*, 5599−5601.
Miziorko, H. M., & Sealy, R. C. (1980) *Biochemistry 19*, 1167−1172.
Miziorko, H. M., & Lorimer, G. H. (1983) *Annu. Rev. Biochem. 52*, 507−535.
Morrow, J. S., Keim, P., Visscher, R. B., Marshall, R. C., & Gurd, F. R. N. (1973) *Proc. Natl. Acad. Sci. U.S.A. 70*, 1414−1418.
Morrow, J. S., Keim, P., & Gurd, F. R. N. (1974) *J. Biol. Chem. 249*, 7484−7494.
Newman, J., & Gutteridge, S. (1993) *J. Biol. Chem. 268*, 25876−25886.
O'Leary, M. H., Jaworski, R. J., & Hartman F. C. (1979) *Proc. Natl. Acad. Sci. U.S.A. 76*, 673−675.
Olejniczak, E. T., Vega, S., & Griffin, R. G. (1984) *J. Chem. Phys. 81*, 4804−4817.
Pierce, J., & Reddy, G. S. (1986) *Arch. Biochem. Biophys. 245*, 483−493.
Pierce, J., Tolbert, N. E., & Barker, R. (1980) *Biochemistry 19*, 934−942.
Rosichan, J. L., & Huffaker, R. C. (1984) *Plant Physiol. 75*, 74−77.
Schneider, G., Lindqvist, Y., Branden, C.-I., & Lorimer, G. H. (1986) *EMBO J. 5*, 3409−3415.
Schneider, G., Lindqvist, Y., & Lundqvist, T. (1990) *J. Mol. Biol. 211*, 989−1008.
Servaites, J. C. (1985a) *Arch. Biochem. Biophys. 238*, 154−160.
Servaites, J. C. (1985b) *Plant Physiol. 78*, 839−843.
Simpson, S. A., Lawlis, V. B., & Mueller, D. D. (1983) *Phytochemistry 22*, 1121−1125.
Wishnick, M., Lane, M. D., & Scruton, M C. (1970) *J. Biol. Chem. 245*, 4939−4947.
Yokota, A., Higashioka, M., & Wadano, A. (1991) *J. Biochem. (Tokyo) 110*, 253−256.

BI942663X